AIAA 81-4308

Robust Flight Control: A Design Example

S. Norman Franklin*
Systems Control Technology, Inc., Palo Alto, Calif.
and
Juergen Ackermann†
DFVLR Oberpfaffenhofen, Wessling, West Germany

A novel parameter space method is used as a tool for the design of a robust stabilization system for the short-period longitudinal mode of a fighter aircraft. The example is an F-4E with additional horizontal canards. Robustness is achieved, in the sense that military specifications for damping and natural frequency are satisfied, by a constant controller in spite of perturbations. The perturbations are changing flight conditions and undetected sensor failures. The resulting controller structure requires two gyros and one accelerometer. The system, including actuator dynamics and feedback dynamics, is of sixth order and, in the design, four free controller parameters have been assumed. Practical considerations are taken into account, such as bandwidth limitation below structural vibration frequencies, actuator limitations, and relaxed emergency specifications in failure situations.

Nomenclature

N_z = normal acceleration
q = pitch rate
$\boldsymbol{x}$ = state vector = $[N_z q \delta_e]^T$
δ_e = deviation of elevator deflection from trim position
ω_{sp} = short-period natural frequency
ζ_{sp} = short-period damping

Introduction

A NEW tool for the design of robust control systems was introduced recently.[1] Parallel to the theoretical development of this so-called "$\mathcal{K}$-space design," a simplified flight control problem was studied and the results are presented in this paper.

Control theory does not provide general design methods for the control of a nonlinear, elastic aircraft. Thus, the control system design is performed with simplified linear models and refined in simulations. The $\mathcal{K}$-space method applied in this paper is a tool to find admissible sets of parameters in an assumed controller structure. The following assumptions are made:

1) Structural vibrations are not included in the design model. However, the control system bandwidth is limited, in order to avoid excitation of structural modes.

2) The aircraft dynamics are linearized for small deviations from stationary flight. Lateral and longitudinal motion are separated. Thus, all results are only necessary, not sufficient, for the stability of the aircraft.

3) Only the short period longitudinal mode is considered in this design example, i.e., second-order dynamics. The actuator is modelled as a first-order low pass with transfer function $14/(s+14)$, its state variable is the deviation of the elevator deflection from its trim position. It is not fed back, because this would require an estimate of the trim position.

4) In order to simplify the design for robustness with respect to accelerometer and gyro failures, the state equations are written in sensor coordinates, i.e., the state vector is $\boldsymbol{x}^T = [N_z q \delta_e]$. Thus

$$\dot{\boldsymbol{x}} = A\boldsymbol{x} + \boldsymbol{b}u$$

$$A = \begin{bmatrix} a_{11} & a_{12} & a_{13} \\ a_{21} & a_{22} & a_{23} \\ 0 & 0 & 14 \end{bmatrix} \qquad \boldsymbol{b} = \begin{bmatrix} b_1 \\ 0 \\ 14 \end{bmatrix} \tag{1}$$

The design example was an F-4E with additional horizontal canards, see Fig. 1. Data for four typical flight conditions were taken from Ref. 2 and are given in the Appendix. The eigenvalue locations of the short period mode are given in Table 1.

The aircraft is unstable in subsonic flight, and insufficiently damped in supersonic flight, such that adequate handling properties must be provided by the control system. Note that in stationary flight the elevator and canard are not used independently. The commanded deflections are coupled as

$$\delta_{e\text{com}} = u \qquad \delta_{c\text{com}} = -0.7\,u$$

where the factor -0.7 was chosen for minimum drag. Thus, the short-period mode stabilization is a single-input problem.

5) Actuator constraints on $|u|$ and $|\dot{u}|$ are not formulated as hard boundaries. However, in the selection of a design point from the admissible set of solutions, the required max $|u|$ should be kept small.

6) The required closed-loop eigenvalue locations are given by military specifications for flying qualities of piloted airplanes.[3] For the short period mode described by

$$s^2 + 2\zeta_{sp}\omega_{sp}s + \omega_{sp}^2 = 0 \tag{2}$$

the restricted range of damping and natural frequency is

$$0.35 \le \zeta_{sp} \le 1.3 \qquad \omega_a \le \omega_{sp} \le \omega_b \tag{3}$$

for normal operating conditions, and

$$0.15 \le \zeta_{sp} \qquad \omega_c \le \omega_{sp} \tag{4}$$

for emergency conditions, where ω_a, ω_b, and ω_c depend on the flight condition, are given in the Appendix for the four conditions considered here. Figure 2 shows the nominal region Γ_j, Eq. (3), together with the open-loop eigenvalues for a subsonic flight condition j. Damping greater than 1 in Eq. (3) corresponds to two real eigenvalues. Equation (3) would admit some real pairs of poles with one of them outside the region Γ_j. In the following, no use is made of this possibility

Received July 31, 1980; revision received April 7, 1981.

*Engineer.

†Director of DFVLR-Institut fuer Dynamik der Flugsysteme.

Table 1 Flight conditions and corresponding open-loop eigenvalues

Flight condition (FC)	Mach no.	Altitude, ft	Open-loop short-period eigenvalues	
1	0.5	5000	−3.07	1.23
2	0.85	5000	−4.90	1.78
3	0.9	35,000	−1.87	0.56
4	1.5	35,000	$-0.87 \pm j4.3$	

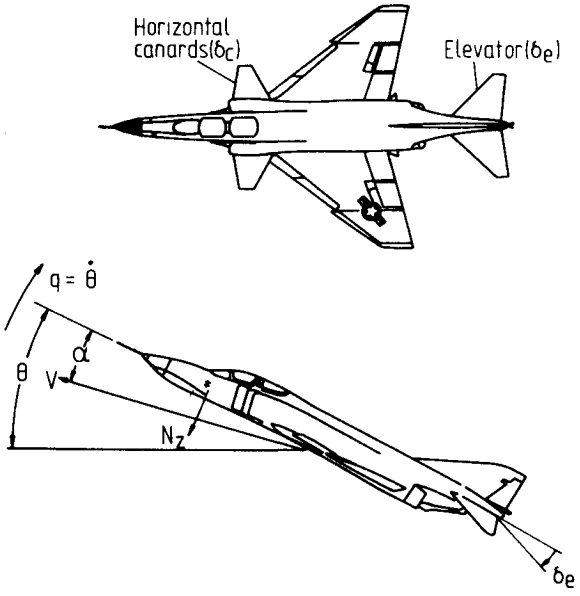

Fig. 1 F-4E with horizontal canards.

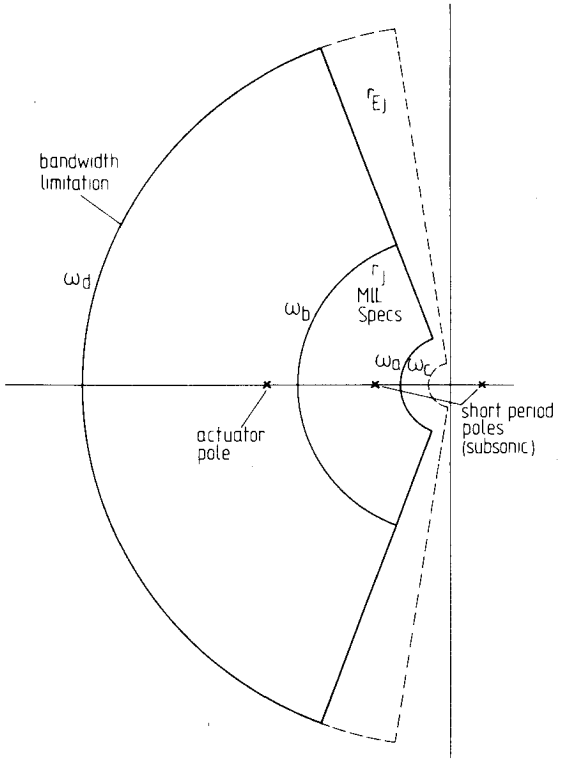

Fig. 2 Flight condition j. Short-period poles must be shifted into Γ_j. Nonshort-period poles s_i such that $\omega_b < |s_i| < \omega_d$, and damping >0.35. All poles in emergency region γ_{Ej} after two sensor failures.

because $\mathcal{K}$-space design assumes a boundary $\omega = \omega(\sigma)$. For all real pairs inside Γ_j, Eq. (3) is satisfied. We require that the closed-loop short-period poles of each flight condition $j = 1, 2, 3, 4$, are located in the respective region Γ_j.

7) The military specifications do not contain requirements for the location of additional closed-loop poles originating from actuator or feedback dynamics. Quick response is essential for a fighter, therefore, the non-short-period eigenvalues should not unnecessarily slow the dynamic response. In order to keep them fast enough, and separate from the short-period eigenvalues, an additional region to the left of Γ_j is prescribed. The damping-requirement $\zeta \geq 0.35$ is kept from Eq. (3), and a natural frequency range $\omega_b \leq \omega \leq \omega_d$, $\omega_d = 70$ rad/s is chosen in the first design step, in order to maintain a bandwidth limitation. It is desirable to reduce ω_d further, since the first structural mode is at approximately 85 rad/s. The extended region is shown in Fig. 2. Plotted in dashed lines is the emergency region Γ_{Ej}, Eq. (4), for which no distinction between different eigenvalues is made, and ω_d is chosen as before.

8) The assumed type of sensor failure is that the nominal gain $v = 1$ is reduced to some value $0 \leq v \leq 1$, and an additional bias or noise term is added at the sensor output. As far as eigenvalue location is concerned, only the multiplicative error by gain reduction is important. It is desired that, after failure of any one sensor, the eigenvalues remain in Γ_j for all flight conditions $j = 1, 2, 3, 4$, and in Γ_{Ej} after any two sensor failures. Since the open-loop does not meet the emergency requirement, at least three sensors are needed. This may be any combination of gyros and accelerometers. This robustness, with respect to sensor failure, guarantees that no instability occurs immediately after the failure. Failure detection may still be necessary to remove the additive error of a failed sensor, however this is not vital for stabilization and may be performed in a time scale, which depends on the magnitude of the additive error. A safe decision with low probability of false alarms will be fast for a full scale output and slow if the sensor sticks at the last indicated value.

The objective of this paper is to investigate how well such requirements can be met using a fixed-gain controller. The simplest controller structure would be static output feedback

$$u = -[k_{Nz} \;\; k_q \;\; 0]x \tag{5}$$

If necessary, dynamic feedback may be used. The design philosophy is that gain scheduling, adaptive control, and redundancy management may be used at a higher hierarchical level, with slower dynamics, if this is necessary to achieve higher performance. The basic level or back-up system, however, should be an extremely simple fixed-gain robust control system. In addition to eigenvalue requirements, the step response also has to meet some inequality constraints. In Ref. 2, bounds are specified for the step response of the output variable

$$C^* = (N_z + 12.43\, q)/C_\infty \tag{6}$$

where the stationary value, C_∞, is used for normalization. In the present problem, it was easy to meet this requirement in a final design step by a prefilter at the pilot input.

Very few university courses teach such design considerations. We have to look into the practice of aircraft companies to learn how valuable the control engineer's tool box is. Some observations are:

1) Linear quadratic design approach is useful to reduce implicitly the required control magnitude $|u|$. In continuous time, and with full-state measurement without observer, it guarantees gain and phase margins.

2) Bode diagrams are convenient to achieve gain and phase margins, and a bandwidth limitation below the frequency range of structural vibrations. Thus, robustness with respect to modelling inaccuracy at high frequencies is achieved.

3) Root locus design is helpful to meet the pole region requirement.

It is more the designer's experience than the quality of these tools that makes a good design. In fact, none of these tools is really good for all aspects of the problem. Robustness, with respect to changing flight condition, is usually achieved by designs for some typical altitudes and speeds, and interpolation between these feedback gains via gain scheduling. The control engineer usually requires that the sensors must not fail, i.e., gyro and accelerometer are quadruplexed, and fast and reliable failure detection is vital for stabilization. It may be conjectured that better solutions exist, since the short-period mode is observable by one gyro or one accelerometer alone.

In this paper, a novel design tool for constant robust controllers is applied, namely $\mathcal{K}$-space design.[1] Its development was motivated by problems of the type described above. In the next section, this method is briefly reviewed, then a design for robustness with respect to different flight conditions is shown, and finally the system is redesigned for robustness with respect to gyro and accelerometer failures.

Pole Region Assignment

The most essential aspect of $\mathcal{K}$-space design is pole region assignment.[1] Other features will be discussed later using the design example. If a tradeoff with other design requirements has to be made, it is not satisfactory to find *one* solution, for which all eigenvalues are in their respective regions in s-plane, e.g., by pole placement or root locus techniques. It is desirable to find *all* such solutions. This is achieved by mapping the region Γ in s-plane into a region P_Γ in the parameter space $\mathcal{P}$ of coefficients of the desired characteristic polynomial first. Then P_Γ is mapped into a corresponding region K_Γ in the parameter space of feedback gains. The first step only deals with properties of polynomials.

$$P(s) = p_0 + p_1 s + \ldots + p_{n-1} s^{n-1} + s^n$$

$$= [p^T \; 1]\,[1 \; s \ldots s^n]^T = \prod_{i=j}^{n} (s - s_i) \tag{7}$$

The problem is: Find the region P_Γ in $\mathcal{P}$-space, such that $p^T \in P_\Gamma$ if, and only if, $s_i \in \Gamma$ for $i = 1,2,\ldots n$. The boundaries of P_Γ, for a connected region Γ with two real axis intersections at σ_L and σ_R, consists of three parts corresponding to the cases that a real eigenvalue crosses the boundary in s-plane at σ_L, or at σ_R, or a complex conjugate pair crosses the complex boundary. For the real values, these boundaries in $\mathcal{P}$-space are the $n-1$ dimensional hyperplanes $P(\sigma_L) = 0$ and $P(\sigma_R) = 0$.

For the complex case

$$P(s) = (s - \sigma - j\omega)\,(s - \sigma + j\omega) \cdot R(s)$$

$$= [s^2 - 2\sigma s + \sigma^2 + \omega^2(\sigma)] \cdot R(s) \tag{8}$$

$\omega^2(\sigma)$ is the complex boundary of the eigenvalue region Γ. The complex boundary may be defined piecewise as in Fig. 2. The complex, and the two real boundaries, partition the $\mathcal{P}$-space into regions distinguished by the location of the eigenvalues relative to Γ. Only that region is of interest for which all eigenvalues are in Γ.

In the second step, a controller structure is assumed, e.g., state feedback

$$u = -k^T x \qquad k^T = [k_1 \; k_2 \; \ldots \; k_n] \tag{9}$$

and the region P_Γ is mapped into a region K_Γ in the controller parameter space $\mathcal{K}$ with coordinates $k_1, k_2 \ldots k_n$ such that $k^T \in K_\Gamma$ if and only if $p^T \in P_\Gamma$. It was shown in Ref. 1, that for state feedback, Eq. (9), this is accomplished by an affine mapping

$$k^T = [p^T \; 1]E \tag{10}$$

where the pole assignment matrix E describing the plant is determined by a controllable pair A, b as follows:

Let

$$R = [b \; Ab \; \ldots \; A^{n-1}b] \qquad e^T = [0 \ldots 0 \; 1]R^{-1}$$

Then

$$E = \begin{bmatrix} e^T \\ e^T A \\ \cdot \\ \cdot \\ \cdot \\ e^T A^n \end{bmatrix} \tag{11}$$

All principal properties of the regions can be studied in the canonical parameter space $\mathcal{P}$. A system (A,b) is interpreted as an affine mapping from $\mathcal{P}$-space to $\mathcal{K}$-space.

For each pair A_j, b_j, a different mapping E_j results, and the solution set is the intersection of the regions $K_{\Gamma j}$ in $\mathcal{K}$-space. Graphical representation of such regions is easy for $n = 2$, and possible for $n = 3$ by computer graphics. For higher system orders the design may proceed stepwise by fixing $n-2$, gains in each step. Also, for output feedback, some gains are fixed.

By Eq. (10), each fixed gain k_i implies a linear relationship $k_i = [p^T 1]\eta_i$, where η_i is the ith column of E. If only two gains remain free, it is convenient to write $P(s)$ as

$$P(s) = R(s) \cdot Q(s)$$

$$= (r_0 + r_1 s + \ldots + r_{n-3} s^{n-3} + s^{n-2})\,(q_0 + q_1 s + s^2)$$

With $r^T = [r_0 r_1 \ldots r_{n-3}]$ this may be written as

$$[p^T \; 1] = [r^T \; 1] \begin{bmatrix} q_0 & q_1 & 1 & & & 0 \\ 0 & q_0 & q_1 & 1 & & \\ & \cdot & & \cdot & \cdot & \\ & & \cdot & & \cdot & \cdot \\ & & & \cdot & & \cdot \\ 0 & & & q_0 & q_1 & 1 \end{bmatrix}$$

$$= [r^T \; 1] \begin{bmatrix} S \\ t^T \end{bmatrix} \tag{12}$$

where S is a $(n-2) \times (n+1)$ matrix and t^T is a $1 \times (n+1)$ vector. Let k_b^T be the fixed gains, which, for convenience, are chosen to be the last $n-2$ gains in k^T. Then

$$k^T = [k_a^T \; k_b^T] = [p^T \; 1]\,[E_a E_b] = [r^T \; 1] \begin{bmatrix} S \\ t^T \end{bmatrix} [E_a \; E_b]$$

We can now express r^T by the known gains k_b^T and q_0, q_1 and substitute this to obtain $k_a^T(q_0, q_1)$.

Explicitly

$$k_b^T = r^T S E_b + t^T E_b$$

$$r^T = (k_b^T - t^T E_b)(S E_b)^{-1}$$

$$k_a^T(q_0, q_1) = (r^T S + t^T) E_a$$

$$= [(k_b^T - t^T E_b)(S E_b)^{-1} S + t^T] E_a \qquad (13)$$

By $k_a^T(q_0, q_1)$ points q_0, q_1 on the boundary of Γ are mapped into the $k_1 - k_2$-plane, where $k_a^T = [k_1 k_2]$. For the real boundaries at σ_L and σ_R, $q_0 + q_1\sigma_L + \sigma_L^2 = 0$ and $q_0 + q_1\sigma_R + \sigma_R^2 = 0$, respectively, and for the complex boundary by Eq. (8), $q_0 = \sigma^2 + \omega^2(\sigma)$ and $q_1 = -2\sigma$.

This tool will be applied to the aircraft example in the next section.

Robustness with Respect to Flight Condition

The first design objective will be to design an output feedback controller, Eq. (5), which meets the nominal pole region requirements at all four flight conditions.

With $r^T = r_0$, $k_b^T = k_3 = 0$, and $E = [\eta_1 \eta_2 \eta_3]$, Eq. (13) becomes

$$[k_{Nz} K_q] = \left\{ -\frac{[0\ q_0\ q_1\ 1]\eta_3}{[q_0\ q_1\ 1\ 0]\eta_3} [q_0\ q_1\ 1\ 0] + [0\ q_0\ q_g\ 1] \right\} \cdot [\eta_1 \eta_2] \qquad (14)$$

For various values of σ first $\omega^2(\sigma)$ on the complex boundary was determined, then $q_0 = \sigma^2 + \omega^2(\sigma)$ and $q_1 = -2\sigma$, and finally $k_{Nz}(\sigma)$ and $k_q(\sigma)$ by Eq. (14). This was plotted in the $(k_{Nz} - k_q)$-plane together with the real boundaries.

The boundary for flight condition 2 is shown in Fig. 3. On a-b, eigenvalues are on the lower natural frequency boundary $\omega_{sp} = 3.5$; on b-c, they are on the damping 0.35 lines. At c, a real root boundary takes over; on c-d, the actuator eigenvalue is at $\sigma = -70$. On d-e, a real short-period eigenvalue is at the upper natural frequency limit $\sigma = -12.6$; and for e-a, the actuator eigenvalue is at $\sigma = -12.6$. The condition for having no real root $\sigma = -3.5$ is satisfied in the total region. This region R_{nom2} is bounded by two straight lines, c-d and d-a, resulting from real root conditions and by the two complex boundary curves a-b and b-c. Note that the boundaries in s-plane are conic sections and, thus, a-b and b-c are segments of conic section also.

The regions $R_{\text{nom1}} - R_{\text{nom4}}$ for the other flight conditions were found by mapping the eigenvalue constraints for each flight condition into the $k_{Nz} - k_q$-plane. These four regions have the intersection R_{nom} shown in Fig. 4. Thus, robustness with respect to changing flight conditions can be achieved by static output feedback of the accelerometer and gyro signals. More precisely, all eigenvalues at all four flight conditions are in their prescribed regions in s-plane if, and only if, the pair k_{Nz}, K_q is chosen in the region R_{nom}.

As an example, choose the design point Q_1, i.e., $k_{Nz} = -0.115$, $k_q = -0.8$. The closed-loop eigenvalues are given in Table 2.

The selection of a design point in R_{nom} is a tradeoff, in which the designer learns which requirements are conflicting, e.g., structural vibrations are most critical in flight condition 2 (high speed, low altitude). They can be reduced by avoiding the vicinity of the $\sigma_2 = -70$ boundary. Low damping is most critical at the supersonic flight condition 4. Damping can be increased by avoiding the vicinity of the $\zeta_4 = 0.35$ boundary. Sluggish responses in landing approach would occur in the vicinity of the $\sigma_1 = -2.02$ boundary. The $\sigma_1 = -7.23$ boundary is only necessary in order to separate actuator and short period poles; the design point may be chosen close to this boundary. Let us assume that the designer wants to

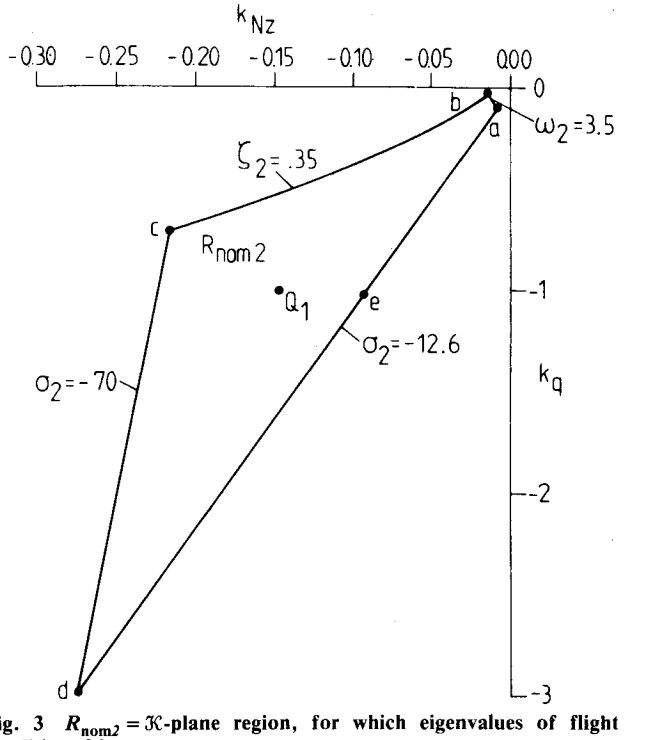

Fig. 3 $R_{\text{nom2}} = \mathcal{K}$-plane region, for which eigenvalues of flight conditions 2 in γ_2.

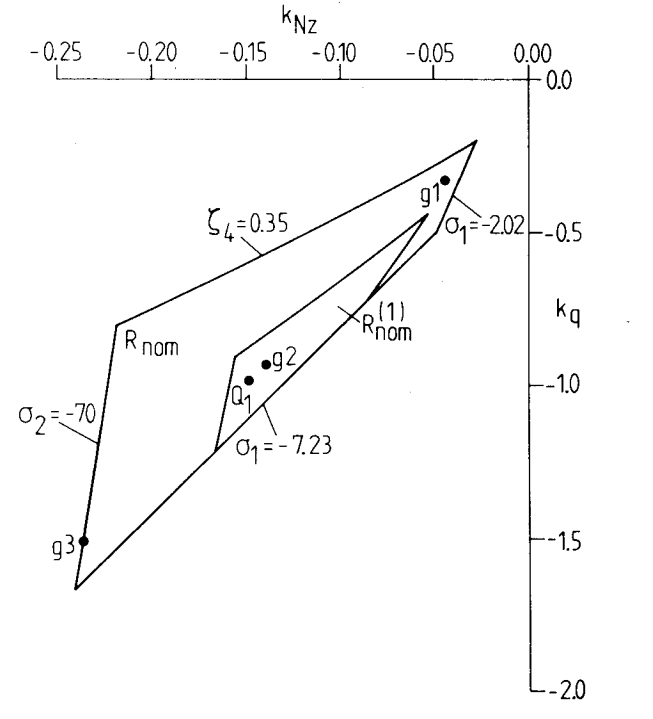

Fig. 4 R_{nom} = intersection of nominal regions for four flight conditions. $R^{(1)}_{\text{nom}}$ = reduced region for tighter bounds. g_1 = small-gain solution, requires smaller $|u|$ than g_2 and g_3, and avoids structural vibration frequencies.

Table 2 Closed-loop eigenvalues for design Q_1

Flight condition (FC)	Short-period eigenvalues		Actuator eigenvalue
	Damping	Natural frequency	
1	0.94	4.68	−18.31
2	0.61	9.18	−37.29
3	0.79	4.63	−17.78
4	0.55	8.11	−27.04

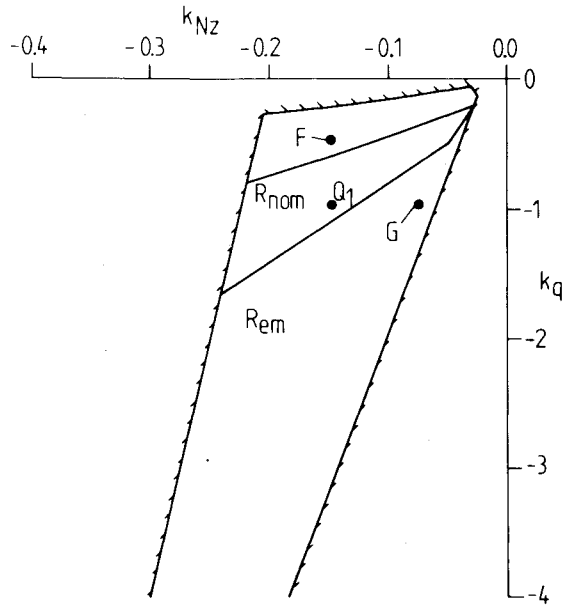

Fig. 5 Nominal region R_{nom} and emergency region R_{em} do not intersect the axes $k_q = 0$ or $k_{Nz} = 0$.

tighten the eigenvalue location regions. Figure 5 shows the reduced region $R^{(1)}_{nom}$, where the high-frequency limit has been lowered from 70 to 50 rad/s, the minimum damping has been increased to 0.5 and the minimum short-period frequency has been increased by 50% for each flight condition. Any gain chosen from $R^{(1)}_{nom}$, would meet these tighter requirements at all four flight conditions.

Another design aspect is the actuator constraint. The maximum required $|u|$ satisfies

$$|u| = |\boldsymbol{k}'\boldsymbol{x}| \leq \|\boldsymbol{k}\| \cdot \|\boldsymbol{x}\| \tag{15}$$

$|u|$ is kept small by choosing a small $\|\boldsymbol{k}\|$, i.e., a design point close to the origin. This design aspect is further illustrated by some simulations for the points g_1, g_2, and g_3 in Fig. 4. For a pilot input filter $1/(s+6)$ the corresponding C^* step responses, and elevator deflections δ_e, are shown in Fig. 6. It is seen that by going from g_2 to g_1 the maximum $|u|$ is reduced by 50%. Such a low gain solution also reduces the effect of sensor noise, i.e., feedback of $\boldsymbol{k}^T(\boldsymbol{x}+\Delta\boldsymbol{x})$ instead of $\boldsymbol{k}^T\boldsymbol{x}$. The safety margin of g_1 from the boundary provides robustness with respect to inaccurate controller implementation $\boldsymbol{k}^T+\Delta\boldsymbol{k}^T$ instead of $\boldsymbol{k}^T$. g_1 is a "soft control" solution; for a fighter, g_2 may be more desirable.

Robustness with Respect to Sensor Failures

As far as stability is concerned, a failure of the accelerometer (gyro) is equivalent to a reduction of $k_{Nz}(k_q)$ from the nominal value to zero or some value in between. Figure 4 shows that the nominal region does not intersect the axes, thus it is not possible to maintain nominal specifications after either failure. Even the emergency region, shown in Fig. 5, does not intersect with the axes. In this, and all following figures, all regions are intersections for the four flight conditions.

The simplest idea would be to use two paralleled accelerometers and two paralleled gyros as in Fig. 7. Taking Q_1 in Fig. 5 as the nominal design point, the 50% gain reduction points F and G are in the emergency region. This solution, however, requires four sensors.

A general dynamic feedback structure was assumed in Ref. 1. This, however, increases the number of free design parameters significantly. Therefore, a more heuristic approach was taken here to introduce feedback filters. The basic idea is to replace one of the accelerometers (gyros) in Fig. 7 by

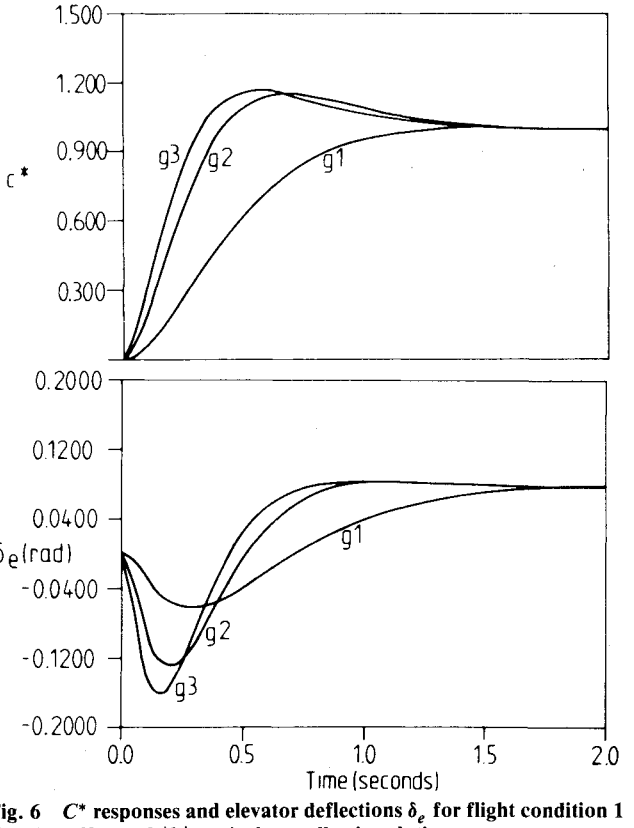

Fig. 6 C^* responses and elevator deflections δ_e for flight condition 1 showing effects of $|k|$. g_1 is the small gain solution.

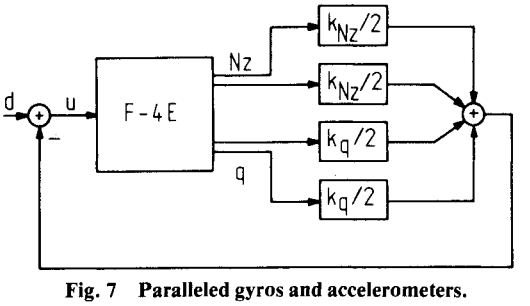

Fig. 7 Paralleled gyros and accelerometers.

an estimate $\hat{N}_z(\hat{q})$ of $N_z(q)$ generated by the gyro (accelerometer). Observers are not particularly useful for the following reasons:

1) If we want to avoid the additional difficulties of an adaptive observer, we have to use a fixed-gain observer, for which separation holds only for one particular flight condition.

2) After sensor failure, u is still fed into the observer, thus for the accelerometer (gyro) failure case, the three gains multiplying $\hat{N}_z$, $\hat{q}$, q (N_z, $\hat{N}_z$, q) must be considered in the design.

Therefore, feedback dynamics are introduced in the form of two stable filters connected to N_z and q. This results in the structure of Fig. 8. A suggestion of Kreisselmeier[4] is to choose filter 1 (2) such that the transfer function from u to $\hat{q}(\hat{N}_z)$ is approximately equal to the transfer function from u to $q(N_z)$. Since the transfer functions to the two sensors have the same denominators, this means cancellation of plant zeros by filter poles and their replacement by the zeros of the other channel as filter zeros. Fortunately, the gain ratio is almost constant in all flight conditions, but the zero locations vary, and cancellation can be correct only for one particular flight condition. Thus, in any case $k_1 = k_4 = K_{Nz}/2$ and $k_2 = k_3 = k_q/2$ is only an initial guess, and a redesign in the four dimensional parameters pace with coordinates k_1, k_2, k_3, and k_4 is necessary.

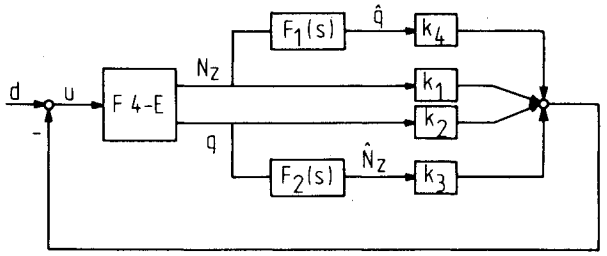

Fig. 8 Dynamic output feedback with filters $F_1(s)$, $F_2(s)$.

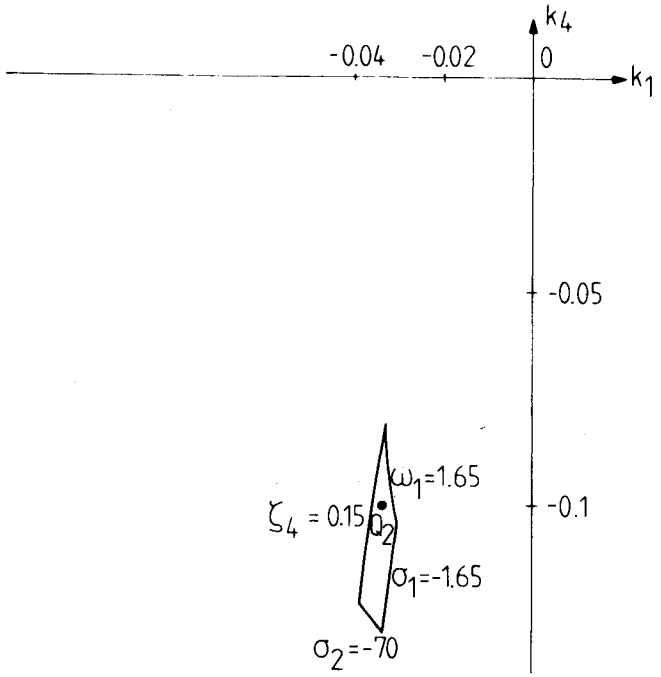

Fig. 9 Emergency region for gyro failure.

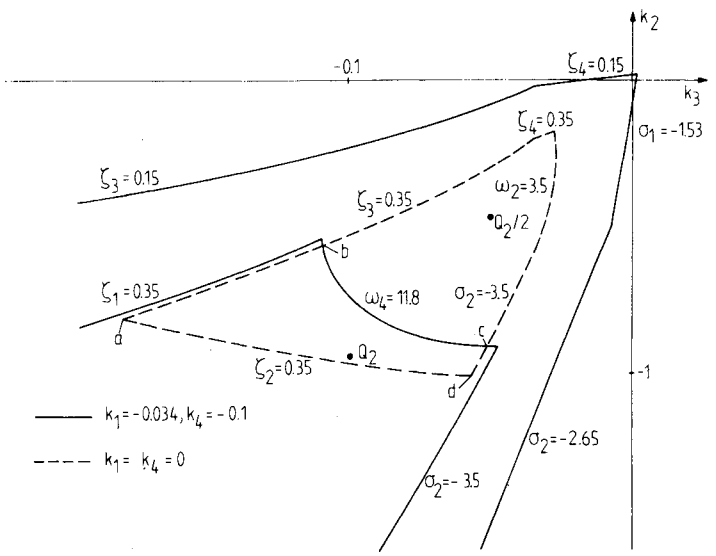

Fig. 10 Two-dimensional cross sections of four-dimensional region in $\mathcal{K}$-space.

The cancellation idea, applied to averaged zero locations of the q-channel, leads to a transfer function

$$F_2(s) = 0.543 \frac{s^2 + 1.172s + 49.9}{(s+0.98)} \cdot \frac{10}{s+10} \tag{16}$$

The term $10/(s+10)$ was included in order to make the filter realizable. It will be shown that this filter produces the expected results for accelerometer failure.

The zeros approximately cancelled by $s+0.98$ varied from -1.57 to -0.637 on the negative real axis. Thus, the filter pole at $s=-0.98$ is weakly controllable from u and, therefore, remains almost unchanged by feedback. The resulting closed-loop pole in the neighborhood of $s=-0.98$ was exempted from the eigenvalue constraint, because it has little effect on the time response.

The same recipe did not work for $F_1(s)$, which, except for the term $10/(s+10)$, is the inverse of $F_2(s)$. Here the approximate cancellation of $s^2+1.172\,s+49.9$ occurs close to the imaginary axis, such that almost undamped oscillations were introduced by inaccurate cancellation. Since eigenvalue locations will be studied exactly in the (k_1,k_2,k_3,k_4)-parameter space, another filter also may be used for producing an independent feedback signal, which is significantly different in phase from N_z. In order to achieve a 90 deg phase advance at low frequencies, rate feedback was chosen with a filter

$$F_1(s) = s/(s+15) \tag{17}$$

With feedback dynamics fixed by Eqs. (16) and (17), a state space representation of the control system is:

$$\frac{\mathrm{d}}{\mathrm{d}t}\begin{bmatrix} N_z \\ q \\ \delta_e \\ w_1 \\ w_2 \\ w_3 \end{bmatrix} = \begin{bmatrix} a_{11} & a_{12} & a_{13} & 0 & 0 & 0 \\ a_{21} & a_{22} & a_{23} & 0 & 0 & 0 \\ 0 & 0 & -14 & 0 & 0 & 0 \\ 0 & 21.79 & 0 & 0 & -9.8 & 0 \\ 0 & -5.331 & 0 & 1 & -10.98 & 0 \\ 1 & 0 & 0 & 0 & 0 & -15 \end{bmatrix} \times \begin{bmatrix} N_z \\ q \\ \delta_e \\ w_1 \\ w_2 \\ w_3 \end{bmatrix} + \begin{bmatrix} b_1 \\ 0 \\ 14 \\ 0 \\ 0 \\ 0 \end{bmatrix} u$$

$$u = -[k_1k_2k_3k_4] \begin{bmatrix} 1 & 0 & 0 & 0 & 0 & 0 \\ 0 & 1 & 0 & 0 & 0 & 0 \\ 0 & 0.543 & 0 & 0 & 1 & 0 \\ 1 & 0 & 0 & 0 & 0 & -15 \end{bmatrix} \begin{bmatrix} N_z \\ q \\ \delta_e \\ w_1 \\ w_2 \\ w_3 \end{bmatrix} \tag{18}$$

Parameter space design was performed in the following sequence of two-dimensional cross sections of the four-dimensional parameter space $\mathcal{K}$:

1) Gyro failure case, i.e., $k_2=k_3=0$. Fixing k_1 and k_4.

2) Accelerometer failure case, i.e., $k_1=k_4=0$. Admissible k_2-k_3-region in this plane.

3) Unfailed case with k_1 and k_4 fixed by step 1. Admissible k_2-k_3-region in this plane. Intersection with result of step 2.

4) Inclusion of a third sensor, here a parallel gyro.

In the gyro failure case, $k_2=k_3=0$, there is no intersection of the nominal regions of all four flight conditions, the intersection of the emergency regions is shown in Fig. 9. Since this region does not allow much variation of k_1 and k_4, the values $k_1=-0.034$, $k_4=-0.1$ were fixed (Q_2 in Fig. 9). For the accelerometer failure case, $k_1=k_4=0$, the nominal region is shown in Fig. 10 in dashed lines.

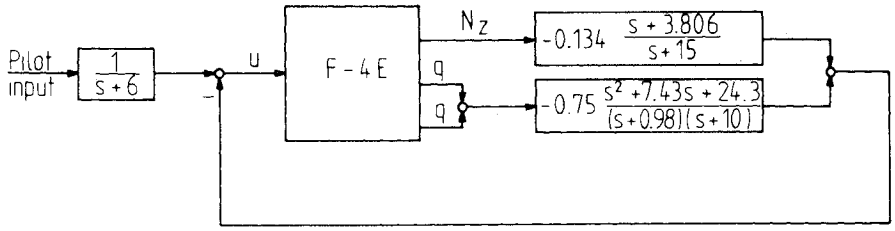

Fig. 11 Final controller configuration, with two gyros and one accelerometer.

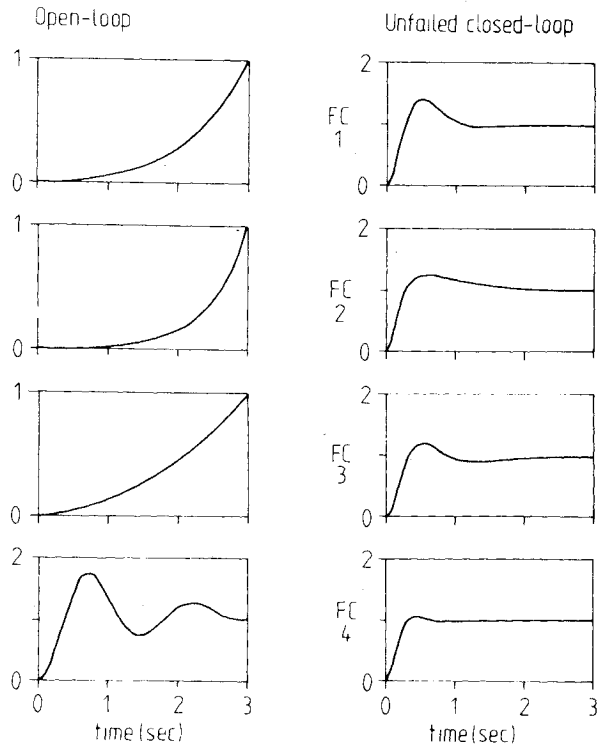

Fig. 12a C^* responses for the open-loop and unfailed closed-loop systems.

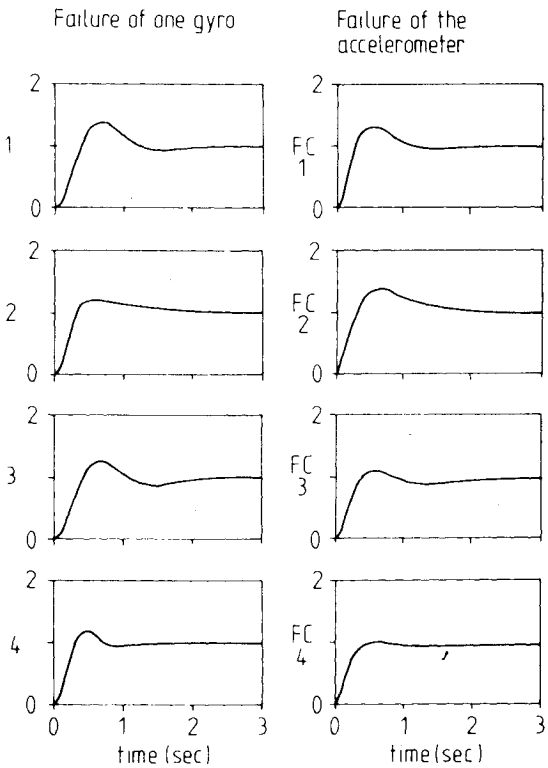

Fig. 12b C^* responses after failure of one sensor.

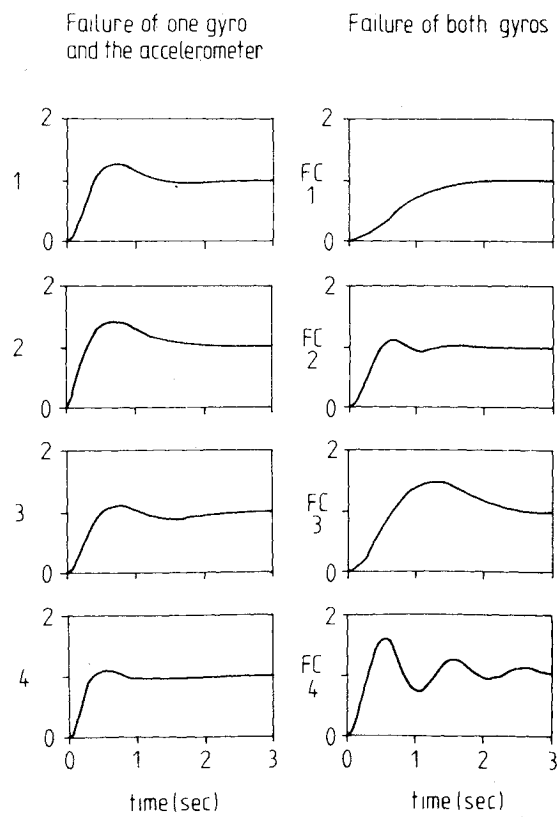

Fig. 12c C^* responses after failure of two sensors.

In the unfailed case, we look at the two-dimensional cross section $k_1 = -0.034$, $k_4 = -0.1$. The resulting nominal and emergency regions for k_2 and k_3 are shown in solid lines in Fig. 10. In the intersection, with vertices a, b, c, d, the nominal specifications are satisfied in the unfailed case and after accelerometer failure.

The desired property, that the system maintains nominal conditions after any one sensor failure, cannot be met in the assumed controller structure, if the remaining sensors are accelerometers. The effect of two paralleled gyros can be discussed by Fig. 10. The gain reduction now occurs simultaneously in k_2 and k_3. Let $k_2 = -0.957$, $k_3 = -0.1$, i.e., point Q_2 in Fig. 10. The 50% gain reduction point $Q_2/2$ is inside the emergency region. It is beyond the $\omega_4 = 11.8$ boundary of the nominal region. Thus, at least in flight condition four, the separation between short-period and nonshort-period modes is not maintained.

Point Q_2 with $k^T = [-0.034 \quad -9.957 \quad -0.1 \quad -0.1]$ was selected. In addition to this nominal case, the following failure situations have been considered:

1) Failure of one gyro:

$$k^T = [-0.034 \quad -0.4785 \quad -0.05 \quad -0.1]$$

2) Failure of the accelerometer:

$$k^T = [0 \quad -0.957 \quad -0.1 \quad 0]$$

3) Failure of one gyro and the accelerometer:

$$k^T = [0 \quad -0.4785 \quad -0.05 \quad 0]$$

4) Failure of both gyros: $k^T = [0.034 \quad 0 \quad 0 \quad -0.1]$

The closed-loop eigenvalues for all cases and flight conditions are given in the Appendix. As designed, the eigenvalues are in their nominal regions in the nominal case, and in the failure cases 2 and 3. They are in the emergency region in case 4. In case 1, FC 2 and 4, the closed-loop poles originating from the actuator, have entered into the region of the short-period eigenvalues. This, however, is no violation of the nominal military specifications. In summary: The military specifications for the short-period eigenvalues are met in all four flight conditions in the nominal case, in both cases of a single sensor failure, and even in the case of accelerometer and gyro failure. For both gyros failed, only emergency conditions are met. This indicates that the gyro is the much more important sensor.

The final controller configuration is shown in Fig. 11. Figure 12 shows the C^* step responses. It is seen here also that, without gyro, it is difficult to find a compromise between sluggish response in landing approach and insufficient damping at high speed and high altitude, i.e., between the $\omega_l = 1.65$ and the $\zeta_6 = 0.15$ boundaries in Fig. 9. The C^* step responses have been shaped by the prefilter at the pilot input, as shown in Fig. 11. They satisfy the bounds given in Ref. 2.

A more detailed version of this paper is available in Ref. 5.

Conclusions

It has been demonstrated that the new $\mathcal{K}$-space design technique can be successfully applied to realistic problems. The resulting flight control system is of sixth order and, for the design, four free controller parameters have been assumed. Four parameter sets for the flight conditions and five controller structures resulting from various failure situations, i.e, $4 \times 5 = 20$ cases, have been considered simultaneously in the design.

In addition to this design method, the result may also be of interest to flight control engineers:

1) For an unstable or insufficiently damped airplane, it was possible to meet the military specifications for a wide range of flight conditions with a constant controller without the usual gain scheduling.

2) Required eigenvalue regions can be made robust with respect to various sensor failures, such that failure detection is not vital for stabilization.

3) The gyro is the most important sensor. In fact, in a later study[6] an alternative solution using three gyros and no accelerometer was given.

Appendix

Table 1A Aerodynamic data for Eq. (1)

	FC 1	FC 2	FC 3	FC 4
Mach =	0.5	0.85	0.9	1.5
Altitude =	5000 ft	5000 ft	35,000 ft	35,000 ft
a_{11}	−0.9896	−1.702	−0.6607	−0.5162
a_{12}	17.41	50.72	18.11	26.96
a_{13}	96.15	263.5	84.34	178.9
a_{21}	0.2648	0.2201	0.08201	−0.6896
a_{22}	−0.8512	−1.418	−0.6587	−1.225
a_{23}	−11.39	−31.99	−10.81	−30.38
b_l	−97.78	−272.2	−85.09	−175.6

Table A2 Military specifications for flying qualities, see Eqs. (3) and (4)

Natural frequency, rad/s	FC 1	FC 2	FC 3	FC 4
ω_a	2.02	3.50	2.19	3.29
ω_b	7.23	12.6	7.86	11.8
ω_c	1.53	2.65	1.65	2.49

Table A3 Closed-loop eigenvalues[a] for the system of Fig. 11

	FC 1	FC 2	FC 3	FC 4
Nominal	(0.64, 4.85)	(0.84, 5.66)	(0.61, 4.98)	(0.77, 6.4)
	(0.78, 12.9)	(0.66, 15.5)	(0.79, 12.3)	(0.66, 13.2)
	−27.6	−48.13	−26.5	−37.1
	−0.89	−1.43	−0.67	−0.88
One gyro failed	(0.52, 4.29)	(0.94, 6.28)	(0.49, 4.4)	(0.91, 7.84)
	(0.89, 9.88)	(0.53, 10.3)	(0.9, 9.76)	(0.45, 8.33)
	−31.76	−55.5	−30.1	−42.5
	−0.89	−1.35	−0.70	−0.91
Accelerometer failed	(0.65, 4.38)	(0.72, 4.62)	(0.62, 4.46)	(0.68, 5.26)
	(0.56, 18.1)	(0.35, 28.3)	(0.60, 16.9)	(0.42, 22.3)
	−15	−15	−15	−15
	−0.87	−1.62	−0.62	−0.86
Accelerometer and one gyro failed	(0.59, 3.66)	(0.69, 4.24)	(0.54, 3.76)	(0.61, 5.48)
	(0.74, 14.7)	(0.50, 20.8)	(0.77, 14.0)	(0.58, 16.5)
	−15	−15	−15	−15
	−0.86	−1.70	−0.61	−0.88
Both gyros failed	(0.80, 1.77)	(0.27, 6.73)	(0.43, 2.34)	(0.16, 6.27)
	−5.78	−3.54	−6.44	−5.35
	−10	−10	−10	−10
	−35.33	−61.43	−33.27	−46.98
	−0.98	−0.98	−0.98	−0.98
All sensors failed (= open loop)	1.23	1.78	0.56	(0.20, 4.4)
	−3.07	−4.90	−1.87	−10
	−10	−10	−10	−14
	−14	−14	−14	−15
	−15	−15	−15	−0.98
	−0.98	−0.98	−0.98	

[a] Complex eigenvalues $s^2 + 2\omega s + \omega^2$ are written (ζ, ω). The short-period eigenvalues are listed first.

Acknowledgments

This work was supported by the U.S. Air Force under Grant AFOSR 78-3633, by the Joint Services Electronics Program under Contract N00014-79-C-0424, and by the Deutsche Forschungs- und Versuchsanstalt fuer Luft- und Raumfahrt (DFVLR), while the second author held a visiting appointment at the Coordinated Science Laboratory, University of Illinois, Urbana-Champaign.

References

[1] Ackermann, J., "Parameter Space Design of Robust Control Systems," *IEEE Transactions on Automatic Control,* AC-25, Dec. 1980, pp. 1058-1072.

[2] Berger, R.L., Hess, Jr., and Anderson, D.C., "Compatibility of Maneuver Load Control and Relaxed Static Stability Applied to Military Aircraft," AFFDL-TR-73-33, April 1973.

[3] "Flying Qualities of Piloted Airplanes," MIL-F-8785B (ASG), Aug. 7, 1969.

[4] Kreisselmeier, G., "Considerations on the Robustness of Control Systems," European Space Agency, Nordwijk, Netherlands, TT-453, May 1978.

[5] Franklin, S.N., "Design of a Robust Flight Control System," M.S. Thesis, Univ. of Illinois, Urbana, 1979; also available in Ackermann, J., Franklin, S.N., Chato, C.B., and Looze, D.P., "Parameter Space Techniques for Robust Control System Design," Univ. of Illinois, Coordinated Science Laboratory, Report R-890, July 1980.

[6] Ackermann, J., "Robust Control System Design," AGARD Lecture Series 109 on Fault Tolerance Design and Redundancy Management Techniques, Athens-Rome-London, Oct. 1980, pp. 9.1-9.14.